

**This is the preprint version of the contribution published as:**

**Ghanem, N., Trost, M., Sanchez Fontanet, L., Harms, H., Chatzinotas, A., Wick, L.Y.**  
(2018):

Changes of the specific infectivity of tracer phages during transport in porous media  
*Environ. Sci. Technol.* **52** (6), 3486 – 3492

**The publisher's version is available at:**

<http://dx.doi.org/10.1021/acs.est.7b06271>

1 **Changes of the Specific Infectivity of Tracer Phages during Transport in Porous Media**

2

3

4

5 Nawras Ghanem<sup>1</sup>, Manuel Trost<sup>1</sup>, Laura Sánchez Fontanet<sup>1</sup>, Hauke Harms<sup>1,2</sup>, Antonis Chatzinotas<sup>1,2</sup>  
6 and Lukas Y. Wick<sup>1\*</sup>

7

8 <sup>1</sup>Helmholtz Centre for Environmental Research - UFZ, Department of Environmental Microbiology,  
9 Permoserstraße 15, 04318 Leipzig, Germany.

10 <sup>2</sup>German Centre for Integrative Biodiversity Research (iDiv) Halle-Jena-Leipzig, Deutscher Platz 5e,  
11 04103 Leipzig, Germany

12

13 Running title: Changes of the Specific Infectivity of Tracer Phages

14

15 Intended for: Environmental Science and Technology.

16

17 \*Corresponding author: Helmholtz Centre for Environmental Research - UFZ. Department of Environmental  
18 Microbiology; Permoserstrasse 15; 04318 Leipzig, Germany. Phone: +49 341 235 1316, fax: +49 341 235 45  
19 1316, e-mail: [lukas.wick@ufz.de](mailto:lukas.wick@ufz.de).

20 **Abstract**

21 Phages (i.e. viruses infecting bacteria) are considered to be good indicators and tracers for fecal  
22 pollution, hydraulic flow or colloidal transport in the subsurface. They are typically quantified as  
23 total virus particles (VLP) or plaque forming units (PFU) of infectious phages. As transport may lead  
24 to phage deactivation, VLP quantification can overestimate the number of infectious phages. In  
25 contrast, PFU counts may underestimate the transport of total virus particles. Using PFU and tunable  
26 resistive pulse sensing-based counting for active and total phages, resp., we quantified the effect of  
27 transport through laboratory percolation columns on the specific infectivity (SI). The SI is defined by  
28 the ratio of total VLP to PFU and is a measure for the minimum particle numbers needed to create a  
29 single infection. Transport of three marine tracer phages and the coli-phage (T4) was described by  
30 colloidal filtration theory. We found that apparent collision efficiencies of active and total counts  
31 differed. Depending on the phage properties (e.g. morphology or hydrophobicity) passage through a  
32 porous medium led to either an increasing or decreasing SI of effluent phages. Our data hence  
33 suggest that both phage mass recovery and the SI should be considered in quantitative phage tracer  
34 experiments.

35

36

37 **One sentence brief.** Transport through a porous medium dynamically changes the specific  
38 infectivity of tracer phages as quantified by particle-to-PFU ratios.

39

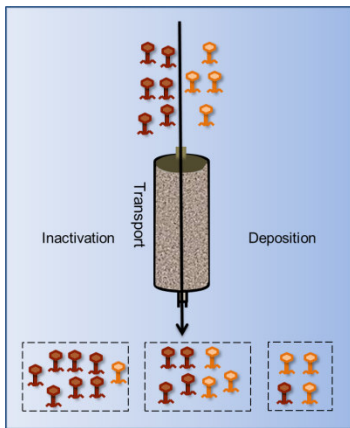
40 **KEYWORDS:** Marine phage, particle-to-PFU ratio, specific infectivity, tracer, transport, qNano.

41

42

43 TOC / Abstract Art

44



45

## 46 INTRODUCTION

47 Bacteriophages (phages) are viruses that infect bacteria. They play an important role in ecological-,<sup>1,2</sup>  
48 and health-related environmental research.<sup>3,4</sup> Phages are considered to be good indicators for the  
49 transport of pathogenic viruses in surface and groundwater.<sup>5,6</sup> Although rarely applied marine phages  
50 hold promise as tracers for hydraulic flow and colloidal transport.<sup>7,8,9</sup> Marine phages are virtually  
51 absent in the terrestrial ecosystem, nonpathogenic and quantifiable with highest sensitivity. It is  
  
52 possible to apply as many as  $10^{15}$  phages ( $\sim 1$  g) in tracer experiments and to detect  $<5$  phages per  
53 mL of recovered water via specific interactions with host bacteria in active count enumeration.<sup>10</sup>  
54 Generally, phage transport is quantified by either total counting of virus-like particles (VLP) or by  
55 assessment of their active counts in a plaque forming unit (PFU) assay.<sup>11,12</sup>  
56 Several studies have analyzed transport-induced virus removal due to deposition and inactivation.<sup>13,14</sup>  
57 Using PFU quantification such research assessed the effect of eluent properties (e.g. beef extract,  
58 sewage, rainwater and others)<sup>15,16</sup> on the release of attached viruses/phages from adsorbent  
59 surfaces.<sup>3,17,18</sup> However, only few studies so far have jointly analyzed total (e.g. using  
60 radioactive<sup>17,19,20,21</sup> or fluorescent-dyed<sup>22</sup> viruses) and active phages. None of them emphasized the  
61 specific infectivity (SI) as a reflection of the probability of suspended VLP to initiate an infection.<sup>23</sup>  
62 The SI can be calculated based on total counts and PFU,<sup>23</sup> and be defined as the minimum particle  
63 numbers needed to create a single infection. A value of 1 indicates that each virus particle is  
64 infective. The SI is thus a measure for the quality of the titer of viruses<sup>24</sup> and can be used to assess  
65 phage dynamics in natural viral lysates. In viral lysates noninfectious particles are often found as a

66 likely result of genome modification (i.e. mutation or damage), failures in the infection cycle<sup>25</sup> or  
67 inactivation.

68 The exclusive use of VLPs counts or quantitative molecular biological techniques (e.g. Bettarel et  
69 al,<sup>26</sup>) may lead to overestimations of the infectivity of virus suspensions. By contrast, as inactivated  
70 phages are not any longer detectable by PFU, results of PFU-based tracer tests (e.g. for hydraulic  
71 water flows or of the quantification of colloidal transport) may be distorted. Virus inactivation  
72 thereby is one of the most important factors controlling virus fate and transport in the subsurface.  
73 The impact of many environmental factors on virus inactivation has been tested. This included the  
74 ionic strength, variations of pH and temperature,<sup>27,28</sup> the clay mineral structures,<sup>29,30</sup> the presence of  
75 liquid-air-interface,<sup>31</sup> types of soil<sup>32</sup> and sand, or the nature and initial concentration of the phages  
76 used.<sup>33</sup> No study however has analyzed the effects of phage properties (i.e, morphology and  
77 hydrophobicity) and transport on SI and associated errors.

78 In the frame of the Collaborative Research Centre AquaDiva<sup>34</sup> (<http://www.aquadiva.uni-jena.de/>)  
79 we here utilized three marine and one coli tracer phage (T4) that belong to two different virus  
80 families (*Siphoviridae* and *Myoviridae*) and vary in their physicochemical surface properties. Active  
81 and total counts were quantified by PFU and tunable resistive pulse sensing (TRPS), respectively.  
82 The TRPS technology uses the coulter principle on the nanoscale and was chosen due to its relative  
83 sensitivity, since it measures particle-by-particle, the possibility to adjust the size range of the  
84 particles counted and its relatively low price. TRPS and PFU counts allowed us to investigate the  
85 effect of transport on the SI of phages in laboratory percolation columns while simultaneously  
86 describing phage deposition and transport by colloidal filtration theory approaches.

87

88

## 89 **EXPERIMENTAL PROCEDURES**

### 90 **Material and Methods**

91 **Propagation of phages and their hosts:** Three lytic marine phages and a common coli-phage used in  
92 our earlier work<sup>9</sup> were used (Table 1). Marine phages PSA-HS2 and PSA-HM1 and their hosts  
93 strains were kindly provided by Dr. B. M. Duhaime (University of Michigan, USA). Phage  
94 vB\_PspS-H40/1<sup>35</sup> together with its host strain was obtained from Dr. J. Zopfi (University of Basel,  
95 Switzerland). The well-characterized T4 coliphage<sup>36,37</sup> and its host *E. coli* (Migula 1895) were  
96 purchased from Deutsche Sammlung von Mikroorganismen und Zellkulturen GmbH (DSMZ,  
97 Germany). All phages were propagated using the double agar-layer technique and purified as in a  
98 previous study.<sup>9</sup> Diluted 2216E medium (50 %) was used to grow marine bacterial strains at room  
99 temperature.<sup>38</sup>

100 **Enumeration of phages:** Active phage counts PFU (mL<sup>-1</sup>) were obtained using a modified spotting  
101 plaque assay technique as detailed earlier.<sup>23</sup> The plates of the phage-host pairs were incubated  
102 overnight at room temperature (37°C for *E. coli*). Total phage counts (Phage particles mL<sup>-1</sup>) were  
103 determined by tunable resistive pulse sensing (TRPS) using an Izon qNano Gold (Izon Science  
104 Europe Ltd., Magdalen Centre, The Oxford Science Park, Oxford, UK) particle counter and the Izon  
105 Control Suite Software V3.2. This instrument has been used before to quantify and characterize (e.g.  
106 particle size) viruses and nanoparticles.<sup>39,40,41</sup> For the measurements samples are passed through a  
107 nanopore (Izon Science) induced by varying trans-membrane voltage and pressure.<sup>39</sup> The samples  
108 were analyzed in 100 mM sterile phosphate buffer (PB; 0.87 g L<sup>-1</sup> K<sub>2</sub>HPO<sub>4</sub>, 0.68 g L<sup>-1</sup> KH<sub>2</sub>PO<sub>4</sub>; pH  
109 7). The phage suspension (40 µL) was added to the upper chamber and subsequent the nanopore  
110 stretch and the ionic current were recorded. The numbers of phage particles were calculated and  
111 calibrated using 1.2 × 10<sup>13</sup> particles mL<sup>-1</sup> calibration particles (size of 110 nm) of allowing for a  
112 minimum of 500 particles per event. Izon Control Suite Software V3.2 was used to calculate the size  
113 of phage particles.

114 **Column deposition experiments:** Percolation experiments using 100 mM PB (ionic strength,  $I \approx 0.12$   
115 M) were conducted as presented in previous work.<sup>9</sup> Briefly, glass columns (diameter: 1 cm, length:

116 10 cm) confined at the bottom by a glass frit (pore size: 100 – 160  $\mu\text{m}$ ) were used. Columns were  
117 packed wet with a d50 median particle size of 0.31 mm commercial quartz sand (Euroquarz-group;  
118 porosity of  $\approx 0.4$  (estimated gravimetrically)). The sand gave no detectable background signal in  
119 TRPS-based counting of phages in the column effluents as verified in controls in the absence of  
120 phages. Then  $>8$  pore volumes (PV) of sterilized 100 mM PB were allowed to pass to equilibrate the  
121 columns. In order to account for the sensitivity of the particle counter and to minimize the phage  
122 inactivation rate by applying low concentrations<sup>33</sup> phages suspension of  $10^8$ - $10^{10}$  PFU  $\text{mL}^{-1}$  (in 100  
123 mM PB) were applied. About 8 PV of phage suspensions were pumped from the top to the bottom of  
124 the columns using a peristaltic pump at a hydraulic flow rate of  $Q = 0.7 \times 10^{-4} \text{ m s}^{-1}$  (19.8  $\text{mL h}^{-1}$ ).  
125 During the experiments the phage concentrations in the influent and effluent were quantified at  
126 regular intervals using both enumeration techniques. Data represent averages and standard deviations  
127 of triplicate analyses of samples obtained from either two (phage vB\_PspS-H40/1 and T4 coliphage)  
128 or three (phages PSA-HM1 and PSA-HS2) independent column experiments.

129 **Colloidal stability of phage suspensions:** The colloidal stability of the phage suspensions ( $10^8$ - $10^{10}$   
130 PFU  $\text{mL}^{-1}$  in 5 mL PB (100 mM)) was determined in triplicate by quantifying active and total phage  
131 particles of unstirred suspensions at  $t = 0 \text{ h}$  and  $t = 2 \text{ h}$ . Colloidal stability experiments were  
132 performed in glass vials (30 mL) to best possibly avoid phage inactivation.<sup>42</sup> In order to assess the  
133 effect of sand on stability and infectivity of phage suspensions, identical experiments were  
134 performed in presence of 10 g of sand (described above).

### 135 **Calculations**

136 **Collision efficiency :** The collision efficiency  $\alpha_t$  was calculated by the colloid filtration theory (eq.  
137 1)<sup>43</sup> as the ratio of the experimental single-collector removal efficiency to the predicted single-  
138 collector contact efficiency.

139 
$$(1)$$



140  $\alpha_t$  is the apparent relative affinity of a phage for the packing material and  $\alpha_0$  the hypothetical collision  
 141 efficiency at  $t = 0$ . The collision efficiency of total phages ( $\epsilon$ ) and the apparent collision efficiency of  
 142 active phages ( $\epsilon_a$ ) were calculated from experimental phage breakthrough curves.<sup>44</sup>  $C_t$  is the effluent  
 143 phage concentration,  $C_0$  the influent phage concentration,  $\epsilon$  the porosity of the packed bed,  $a_s$  the  
 144 radius of the sand particles (mean diameter 0.29 mm),  $L$  the length of the column, and  $\eta_{trans}$  the  
 145 predicted single-collector contact efficiency.<sup>44</sup>

146 **Mass recovery (M):** The mass recovery of active ( $M_a$ , eq. 2) and total ( $M_{tot}$ , eq. 3) phage was  
 147 determined by the %-ratio of total phages in the effluent and the influent as quantified either by PFU  
 148 or total VLP enumeration (eqs. 2 & 3) with  $C_{t,a,effluent}$ ,  $C_{t,a,influent}$  and  $C_{t,tot,effluent}$ ,  $C_{t,tot,influent}$  being the  
 149 effluent and influent phage concentrations assessed by PFU and total VLP enumeration, resp..

150 
$$(2)$$

151 
$$(3)$$

152 **Specific Infectivity (SI):** The specific infectivity of the phages at a given time  $t$  ( $\rho$ ) was calculated as  
 153 the particle-to-PFU ratio,<sup>9</sup> i.e. by the ratio of the total phage  $C_{t,tot}$  (VLP mL<sup>-1</sup>) and the active (i.e.  
 154 infectious) phage concentrations  $C_{t,a}$  (PFU mL<sup>-1</sup>) in a sample (eq. 4).

155 
$$(4)$$

156 The relative change of the SI ( $\rho$ ) was determined (Fig. 2) as the ratio of the SI in the effluent ( $\rho_e$ ) and the  
 157 influent ( $\rho_i$ ) at a given time  $t$  (eq.5).

158 
$$(5)$$

159 The time averaged SI of the inflow ( $\rho_i$ ) and effluent ( $\rho_e$ ) were calculated by eqs. 6 & 7 with  $Q$  being the  
 160 hydraulic flow rate (mL h<sup>-1</sup>) in the column.

161 
$$(6)$$

162 
$$(7)$$

163

## 164 RESULTS

165 **Phage Transport in Saturated Percolation Columns.** The transport experiments were conducted  
166 using sand-packed columns under continuous, saturated flow conditions. Three marine phages (PSA-  
167 HM1, vB\_PspSH40/1, PSA-HS2) and one coli phage (T4) of differing morphology, size and  
168 physicochemical surface properties were used (Table 1). All phages exhibited a high colloidal  
169 stability (96-112%) during the observation period (2 h) (Table 1).

170 Infectious and total phage particles in effluent samples were quantified by PFU and TRPS counts at  
171 given time points of the breakthrough curves. Additionally, TRPS allowed us to assess the average  
172 size of the VLP in measured samples. Inspection of breakthrough curves revealed differences  
173 between the mass recoveries of total vs. active phage particles of three of the phages (Figs. 1 & S1).  
174 Only phage vB\_PspSH40/1 showed a similar mass recovery of active and total phages ( $M_{a-p} \approx M_{tot-p} \approx$   
175 30%; cf. Table 1 and eq. 2&3). Mass recoveries of the infectious forms ( $M_{a-p} = 6-50\%$ ) of the other  
176 phages were clearly reduced relative to  $M_{tot-p} = 47-107\%$  of the total phages. The phages T4 ( $M_{tot-p} =$   
177 63%) and PSA-HM1 ( $M_{tot-p} = 107\%$ ) reached high transport efficiencies whereas phages  
178 vB\_PspSH40/1 ( $M_{a-p} = 30\%$ ) and PSA-HS2 ( $M_{tot-p} = 56\%$ ) were generally more retained despite of  
179 efficient transport of phage PSA-HS2 ( $C/C_0 \approx 1$ ) during initial breakthrough (Fig. S1).

180 The differences of the breakthrough of active and total phage particles were also reflected by the  
181 apparent collision efficiencies (Table 1) of active ( and total phages ( for both the initial collision  
182 efficiency ( and once quasi steady state was reached ( . For phages T4 and PSA-HM1 the was three-  
183 to fivefold increased relative to , while of phages vB\_PspSH40/1 and PSA-HS2 the was and about  
184 threefold smaller than , respectively. TRPS measurements revealed a decreased particle sizes of both  
185 PSA-HM1 and T4 phages eluting at later pore volumes (Fig. S3).

186 **Changes of the Specific Infectivity.** The SI was calculated as the particle-to-PFU ratio in samples of  
187 the phage suspensions (eq. 4). The SI of the influent ( $SI_{\text{influent}}$ ) depended on the phage type (Table 1)  
188 and varied from 1.7 (most infectious, PSA-HM1) via 4.2 (PSA\_HS2) and 5.3 (T4) to 10 (least  
189 infectious; vB-PspSH40/1). This means that about 60, 24, 19, and 10% of the total VLP of the  
190 influents of PSA-HM1, PSA-HS2, T4 and vB-PspSH40/1 were infectious (Fig. S2). No changes of  
191 the colloidal stability and the SI of the phages were observed in static batch experiments in the  
192 presence of sand. (Table 1, Fig. S4). Transport in the sand-filled columns however changed the SI of  
193 the phages as was best observed when quasi steady state effluent concentrations of the breakthrough  
194 curves were reached (Fig. 1): While the  $SI_{\text{effluent}}$  of phage vB-PspSH40/1 remained unchanged, the  
195  $SI_{\text{effluent}}$  of the phages PSA-HM1 and T4 increased 2.5- and 9-fold (i.e. 2.5 -9 fold more viruses were  
196 needed to initiate a single PFU in the effluent as compared to the influent).

197 By contrast, in the effluent of phage PSA-HS2 only 2.9 phages were needed to initiate the infection  
198 (cf. Tab.1) as compares to 4.2 in the influent. This points either at a similar transport-induced  
199 decrease of total and active phages (vB-PspSH40/1) or a selective enrichment of active (PSA-HS2)  
200 or inactivated (PSA-HM1, T4) phages (Fig. S1) as also reflected by the mass recovery of total and  
201 active phages (Table 1). Figure 2 shows that the relative changes of the SI ( $\Delta SI$ ) may vary significantly  
202 during a transport experiment. Interestingly,  $\approx 1$  at the front of the breakthrough were observed likely  
203 pointing at straining effects<sup>45</sup> and poor deactivation of phages eluting at the front of the  
204 breakthrough.

## 205 **DISCUSSION**

206 In this study we analyzed the effect of phage properties and transport on the specific infectivity of  
207 phages. Thereby, we evaluated the usefulness of PFU-based phage enumeration approach as a proxy  
208 for the quantification of total phage particle transported. . For this purpose, we studied the  
209 commonly described coli-phage T4 and three marine phages that had been reported to be a good

210 tracers for hydrological flow and colloidal transport.<sup>46,47,9</sup> To our knowledge this is the first study  
211 that simultaneously enumerates active and total phages during transport through porous media. We  
212 found that passage through a porous medium changed the ratios between active and total phage  
213 particle to extents that depended on the individual phages (Fig. 1). This was reflected by distinct  
214 apparent collision efficiencies of active and total phages (Table 1). Observed phage mass recovery  
215 based on PFU counts was in agreement with previous studies<sup>37,9</sup> and revealed lower mass recovery of  
216 phage T4 than PSA-HM1 and PSA-HS2. Using total counts, by contrast, we found high mass  
217 recoveries of colloidal phage particles after passage through a porous medium. The SI depended on  
218 the phages tested and always was  $>1$  (cf. Table 1) and, hence, higher than for many of the phages  
219 reported.<sup>25</sup> Phage-specific differences of the SI are in accordance with earlier studies, showing that  
220 the variations depended on virus type and quantification method.<sup>48, 49,23</sup>

221 **Effect of transport on the Specific Infectivity.** No effects of the suspension buffer on the colloidal  
222 stability and the SI of the phages were observed (Fig. S5). The relative changes of the SI of phages  
223 during transport hence seemed to be driven by both phage deposition and inactivation (Fig. S2).  
224 Known reasons for phage inactivation are the break off of the phage tail or a damage of the capsids  
225 of phages.<sup>50,51,52</sup> This may either lead to changes of the phage particle size, to alterations of the  
226 physico-chemical surface properties and, as a consequence, to differing deposition and transport  
227 properties of active and inactive phages. Smaller phages are generally better transported than bigger  
228 phages,<sup>53,9</sup> while more hydrophobic phages are thought to exhibit a higher (i.e. the phages are more  
229 retained during transport) than more hydrophilic phages.<sup>54,55</sup> If  $>$  consistently lower PFU than total  
230 phage counts were detected in the effluent (cf. phages T4 and PSA-HM1 in Fig. 2). This either  
231 proposes that the retention of active phages was higher than the retention of total phage particles  
232 and/or that transport led to significant deactivation of the phages. PFU-based quantification will in  
233 such cases will underestimate the transport of total phage particles. In case of  $\approx$  (cf. phage vB\_PspS-  
234 H40/1) the inactivation and deposition rates of phage particles are similar and particle transport is

235 suitably reflected by PFU enumeration. Finally, if ,< selective enrichment of PFU in the effluent is  
236 seen (cf. phage PSA-HS2) and PFU-based tracer experiments can overestimate transport of total  
237 phage particles.

238 **Effect of phage properties on the Specific Infectivity.** Several mechanisms control the SI of  
239 phages during transport in porous media. In case of *Myoviridae* phages (i.e. phages T4 or PSA-  
240 HM1) inactivation may be the main driver for our observations. Their (nonflexible) contractile tail  
241 make *Myoviridae* phages more sensitive to inactivation than Siphoviridae (i.e. phages PSA-HS2 or  
242 vB\_PspS-H40/1) with flexible tails. This was reflected by the decrease in size of *Myoviridae* phages  
243 tested whereas no change was recorded for *Siphoviridae* phages (Fig. S3). This is also in accordance  
244 with observations that phages of the *Siphoviridae* family are generally highly resistant to adverse  
245 conditions.<sup>56,52</sup> The physical stress resulting from phage transport in conjunction with strong sand-  
246 phage interactions (as was confirmed by the extended Derjaguin–Landau–Verwey–Overbeek  
247 (XDLVO) calculations in a previous study)<sup>9</sup> may break off the nonflexible tails and lead to phage  
248 inactivation.<sup>50</sup> The higher transport-induced inactivation of phage T4 than of phage PSA-HM1 could  
249 be attributed to its higher hydrophobic affinity to sand than of PSA-HM1. Inactivation is further  
250 supported by the size of the particles recorded by the TRPS revealing clearly decreasing sizes for  
251 both *Myoviridae* yet not for the *Siphoviridae* (Fig. S3). Additional support for deactivation of phages  
252 by transport-induced processes comes from sand batch experiments under static conditions that  
253 showed no significant change of the SI of all phages tested (Fig. S4 and Table S1). This finding is in  
254 agreement with earlier studies that illustrated the role of solid matrices in preventing viruses from  
255 inactivation.<sup>57,33,19</sup> The decreasing relative (eq. 5, Fig. 2) of phage PSA-HS2, however, may only be  
256 explained by preferential attachment of inactivated phages during transport (cf. Fig. S2).

257

258 **Implications for phage transport studies.** Due to the limited sensitivity of the TRPS method and its  
259 inability to discriminate phages from other particles of similar size, PFU enumeration approaches

260 may remain the method of choice in field tracer phage experiments. PFU enumeration thereby  
261 appeals through its high specificity of phage-host interactions and its extremely high sensitivity of  
262 one or two phages mL<sup>-1</sup> of recovered water.<sup>46</sup> Our approach however allows for easy comparison and  
263 calibration of tracer phages for their SI and transport properties and, hence, for better selection and  
264 tailored use of phages as tracers at given environmental conditions. At present, our data do not allow  
265 for the quantitative discrimination of inactivation and deposition rates of active and inactivated  
266 phages. They though show that transport through porous media changes the SI of certain phages and  
267 leads either to a relative enrichment or depletion of infectious phages. Hence, phage properties and  
268 SI should be considered in quantitative tracer experiments. Transport effects on the SI may also be  
269 relevant in health-related phage indicator and tracer studies or during transport of pathogenic viruses:  
270 active viruses may get selectively enriched during transport in porous media, resulting in decreased  
271 specific infectivity and increased risk to potential receptors. Finally, transport-induced selective  
272 enrichment of infectious viruses may further be used to concentrate titers or to produce therapeutic  
273 viruses at high concentrations.

274

#### 275 **ACKNOWLEDGEMENTS**

276 This study is part of the Collaborative Research Centre AquaDiva (CRC1076 AquaDiva) of  
277 the Friedrich Schiller University Jena, funded by the Deutsche Forschungsgemeinschaft and the  
278 Helmholtz Centre for Environmental Research. The authors wish also to thank Jelena Fix, Jana  
279 Reichenbach, Birgit Würz and Luisa Ciabbarri for skilled technical help. The authors further thank  
280 Bärbel Kiesel and René Kallies for helpful discussions.

281

#### 282 **SUPPORTING INFORMATION AVAILABLE**

283 Supporting Information is available and contains four figures and one table.

284

285 **FIGURE CAPTIONS**

286

287 **Figure 1:** Breakthrough curves of total (particles mL<sup>-1</sup>; empty circles) and active (PFU mL<sup>-1</sup>; filled  
288 circles) counts of three marine tracer phages (PSA-HM1, vB\_PspS-H40/1, PSA-HS2) and a  
289 commonly used coli model phage (T4) of sand filled percolation columns. Dashed and long-short  
290 dashed lines reflect total and active phages in the inflow. Please note that the scales of the y-axes  
291 differ.

292

293 **Figure 2:** Time-dependent relative change of the specific infectivity (cf. eqs. 4&5) of three marine  
294 tracer phages and a commonly used non-marine model phage during transport in a sand filled  
295 column. Increasing  $SI_{rel,t}$  refers to a transport-induced phage deactivation while decreasing  $SI_{rel,t}$  point  
296 at a relative enrichment of active phages.

297

**Table 1.** Overview of selected phage characteristics, specific infectivity (eq. 4) of the influent ( $SI_{\text{influent}}$ , eq.6), specific infectivity of the effluent of a complete transport experiment ( $SI_{\text{effluent}}$ , eq. 6) and at quasi steady state effluent concentrations ( $SI_{\text{effluent-p}}$ ), the apparent collision efficiencies (eq. 1) of total ( $\alpha_{\text{tot}}$ ) and active ( $\alpha_a$ ) phages, the apparent mass recovery (eq. 2&) of active ( $M_a$ ,  $M_{a-p}$ ) and total ( $M_{\text{tot}}$ ,  $M_{\text{tot-p}}$ ) phages of a complete transport experiment and at quasi plateau as well as the colloidal stability of phages in suspension. The last column refers to the calculated apparent relative loss due to adhesion.

Phage name (Family name)	Host name	Zeta potential	Water contact angle	Size <sup>a</sup> (Head/tail)	Specific infectivity of influent	Specific infectivity of effluent <sup>a</sup>	Apparent collision efficiency of active phages	Apparent collision efficiency of total phages	Mass recovery of active phages	Mass recovery of total phages	Colloidal stability of active phages (total phages) <sup>e</sup>
		$\zeta^a$	$\Theta_w^a$		$SI_{\text{influent}}$	$SI_{\text{effluent-p}}^b$ ( $SI_{\text{effluent}}$ )	$\alpha_{a-p}^c$ ( $\alpha_{0,a}$ )	$\alpha_{\text{tot}}^c$ ( $\alpha_{0,\text{tot}}$ )	$M_{a-p}^d$ ( $M_a$ )	$M_{\text{tot-p}}^d$ ( $M_{\text{tot}}$ )	(%)
		(mV)	(degree)	(nm)	(VLP/PFU)	(VLP/PFU)	( $\times 10^{-2}$ )	( $\times 10^{-2}$ )	(%)	(%)	(%)
<b>PSA-HM1</b> (Myoviridae)	<i>Pseudoalteromonas H71</i>	-18 ± 1	40 ± 5	173 (60/113)	1.7	4.2 (3.7)	16 ± 4 (12)	5 ± 2 (4)	50 (37)	107 (80)	96 ± 7 (106 ± 11)
<b>T4</b> (Myoviridae)	<i>E. coli</i> ( <i>Migula 1895</i> )	-13 ± 1	95 ± 5	203 (90/113)	5.3	50 (50)	64 ± 5 (67)	11 ± 9 (18)	6 (7)	63 (63)	101 ± 0 (107 ± 5)
<b>vB_PspSH40/1</b> (Siphoviridae)	<i>Pseudoalteromonas H40</i>	-11 ± 3	53 ± 3	111 (42/69)	10	11 (9.1)	15 ± 4 (19)	19 ± 7 (27)	30 (34)	30 (28)	96 ± 17 (99 ± 6)
<b>PSA-HS2</b> (Siphoviridae)	<i>Pseudoalteromonas H13-15</i>	-13 ± 4	40 ± 5	210 (60/150)	4.2	2.9 (2.9)	4 ± 4 (4)	16 ± 7 (23)	89 (75)	56 (47)	112 ± 8 (109 ± 14)

<sup>a</sup> Data taken from <sup>9</sup>; <sup>b</sup> SI (eq. 6 & 7) in the overall effluent ( $SI_{\text{effluent}}$ ) and at quasi steady state effluent concentrations of active and total and phages ( $SI_{\text{effluent-p}}$ ). <sup>c</sup> Average and standard deviations ( $n \geq 8$ ) of the apparent initial collision efficiency of active ( $\alpha_{0,a}$ ) and total ( $\alpha_{0,\text{tot}}$ ) phages: apparent collision efficiency at the quasi steady state effluent concentrations of active ( $\alpha_{a-p}$ ) and total and phages ( $\alpha_{\text{tot-p}}$ ) (cf. eq. 1). <sup>d</sup> Average and standard deviations ( $n \geq 8$ ) of the mass recovery of active and total phages (cf. eq. 2 & 3) of the total breakthrough curves ( $M_a$ ,  $M_{\text{tot}}$ ) and at quasi steady state effluent concentrations ( $M_{a-p}$ ,  $M_{\text{tot-p}}$ ). <sup>e</sup> Colloidal stability determined in batch experiment after 2 h.



310

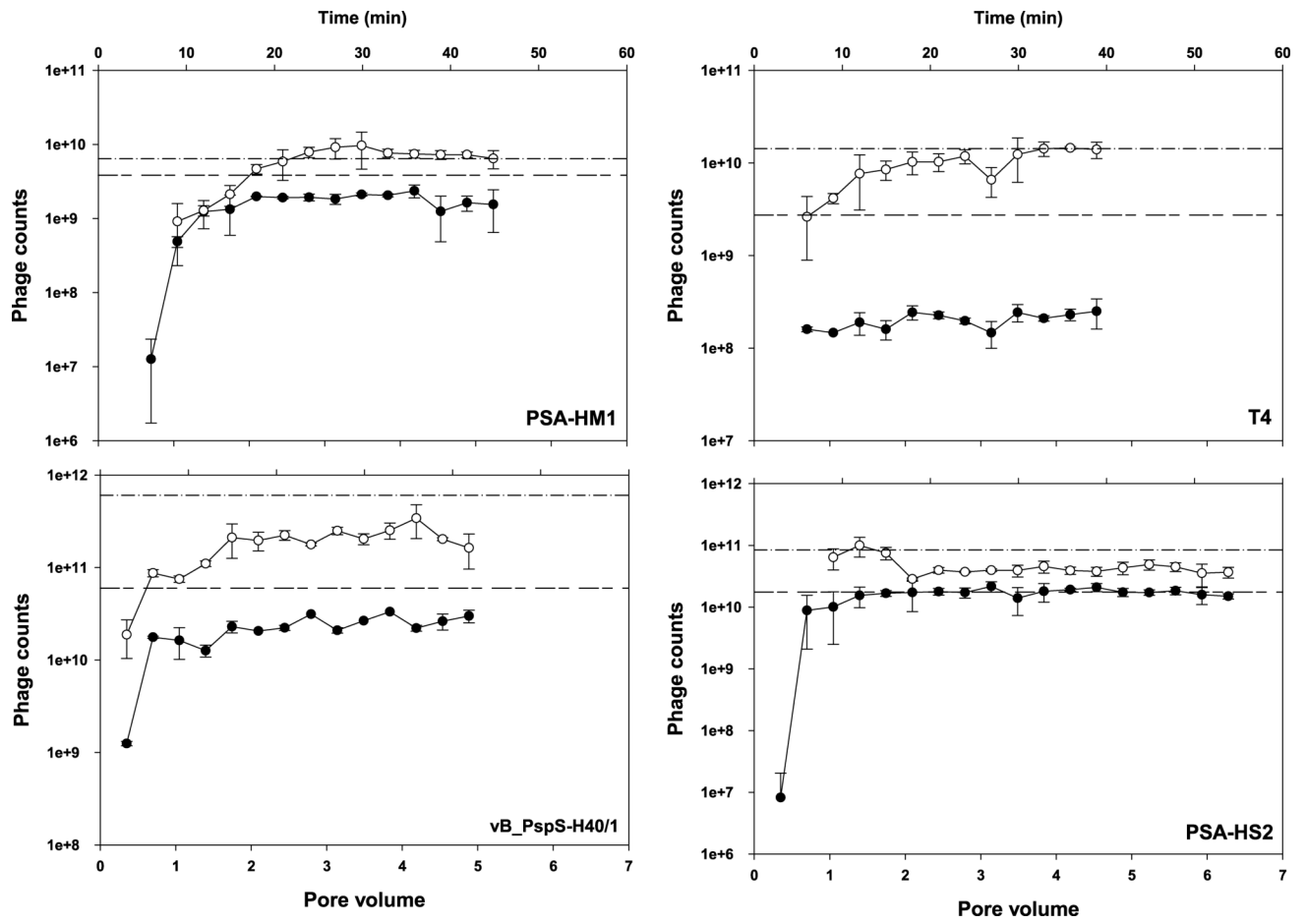
- 311 (1) Williamson, K. E.; Harris, J. V.; Green, J. C.; Rahman, F.; Chambers, R. M. Stormwater runoff drives  
312 viral community composition changes in inland freshwaters. *Front. Microbiol.* **2014**, *5*, 105.
- 313 (2) Rehmann, L. L. C.; Welty, C.; Harvey, R. W. Stochastic analysis of virus transport in aquifers.  
314 *Water Resour. Res.* **1999**, *35* (7), 1987–2006.
- 315 (3) Morales, I.; Atoyan, J.; Amador, J.; Boving, T. Transport of Pathogen Surrogates in Soil Treatment  
316 Units: Numerical Modeling. *Water* **2014**, *6* (4), 818–838.
- 317 (4) Masciopinto, C.; La Mantia, R.; Chrysikopoulos, C. V. Fate and transport of pathogens in a  
318 fractured aquifer in the Salento area, Italy. *Water Resour. Res.* **2008**, *44* (1), W01404.
- 319 (5) Redman, J. A.; Grant, S. B.; Olson, T. M.; Hardy, M. E.; Estes, M. K. Filtration of recombinant  
320 Norwalk virus particles and bacteriophage MS2 in quartz sand: Importance of electrostatic  
321 interactions. *Environ. Sci. Technol.* **1997**, *31* (12), 3378–3383.
- 322 (6) Keswick, B. H.; Wang, D.-S.; Gerba, C. P. The Use of Microorganisms as Ground-Water Tracers: A  
323 Review. *Ground Water* **1982**, *20* (2), 142–149.
- 324 (7) Flynn, R. M.; Schnegg, P.-A.; Costa, R.; Mallen, G.; Zwahlen, F. Identification of zones of  
325 preferential groundwater tracer transport using a mobile downhole fluorometer. *Hydrogeol. J.*  
326 **2005**, *13* (2), 366–377.
- 327 (8) Flynn, R. M.; Mallèn, G.; Engel, M.; Ahmed, A.; Rossi, P. Characterizing Aquifer Heterogeneity  
328 Using Bacterial and Bacteriophage Tracers. *J. Environ. Qual.* **2015**, *44* (5), 1448.
- 329 (9) Ghanem, N.; Kiesel, B.; Kallies, R.; Harms, H.; Chatzinotas, A.; Wick, L. Y. Marine Phages As  
330 Tracers: Effects of Size, Morphology, and Physico–Chemical Surface Properties on Transport in a  
331 Porous Medium. *Environ. Sci. Technol.* **2016**, *50* (23), 12816–12824.
- 332 (10) Rossi, P. Advances in biological tracer techniques for hydrology and hydrogeology using  
333 bacteriophages, Université de Neuchâtel, 1994.
- 334 (11) Wielen, P. W. J. J. van der; Senden, W. J. M. K.; Medema, G. Removal of Bacteriophages MS2 and  
335 ΦX174 during Transport in a Sandy Anoxic Aquifer. *Environ. Sci. Technol.* **2008**, *42* (12), 4589–  
336 4594.
- 337 (12) Nasser, A. M.; Oman, S. D. Quantitative assessment of the inactivation of pathogenic and  
338 indicator viruses in natural water sources. *Water Res.* **1999**, *33* (7), 1748–1752.
- 339 (13) Gerba, C. P.; Lance, J. C. Poliovirus removal from primary and secondary sewage effluent by soil  
340 filtration. *Appl. Environ. Microbiol.* **1978**, *36* (2), 247–251.
- 341 (14) O’Luanaigh, N. D.; Gill, L. W.; Misstear, B. D. R.; Johnston, P. M. The attenuation of  
342 microorganisms in on-site wastewater effluent discharged into highly permeable subsoils. *J.*  
343 *Contam. Hydrol.* **2012**, *142–143*, 126–139.
- 344 (15) Landry, E. F.; Vaughn, J. M.; Thomas, M. Z.; Beckwith, C. A. Adsorption of Enteroviruses to Soil  
345 Cores and Their Subsequent Elution by Artificial Rainwater. *Appl. Environ. Microbiol.* **1979**, *38* (4),  
346 680–687.
- 347 (16) Hurst, C. J.; Gerba, C. P. Development of a quantitative method for the detection of enteroviruses  
348 in soil. *Appl. Environ. Microbiol.* **1979**, *37* (3), 626–632.
- 349 (17) McConnell, L. K.; Sims, R. C.; Barnett, B. B. Reovirus removal and inactivation by slow-rate sand  
350 filtration. *Appl. Environ. Microbiol.* **1984**, *48* (4), 818–825.
- 351 (18) LaBelle, R. L.; Gerba, C. P. Influence of pH, salinity, and organic matter on the adsorption of  
352 enteric viruses to estuarine sediment. *Appl. Environ. Microbiol.* **1979**, *38* (1), 93–101.
- 353 (19) Moore, R. S.; Taylor, D. H.; Sturman, L. S.; Reddy, M. M.; Fuhs, G. W. Poliovirus Adsorption by 34  
354 Minerals and Soils. *Appl. Environ. Microbiol.* **1981**, *42* (6), 963–975.

- 355 (20) Murray, J. P.; Laband, S. J. Degradation of poliovirus by adsorption on inorganic surfaces. *Appl.*  
356 *Environ. Microbiol.* **1979**, *37* (3), 480–486.
- 357 (21) Ryan, J. N.; Harvey, R. W.; Metge, D.; Elimelech, M.; Navigato, T.; Pieper, A. P. Field and  
358 Laboratory Investigations of Inactivation of Viruses (PRD1 and MS2) Attached to Iron Oxide-  
359 Coated Quartz Sand. *Environ. Sci. Technol.* **2002**, *36* (11), 2403–2413.
- 360 (22) Asraf-Snir, M.; Gitis, V. Tracer studies with fluorescent-dyed microorganisms—A new method for  
361 determination of residence time in chlorination reactors. *Chem. Eng. J.* **2011**, *166* (2), 579–585.
- 362 (23) Alfson, K. J.; Avena, L. E.; Beadles, M. W.; Staples, H.; Nunneley, J. W.; Ticer, A.; Dick, E. J.;  
363 Owston, M. A.; Reed, C.; Patterson, J. L.; et al. Particle-to-PFU Ratio of Ebola Virus Influences  
364 Disease Course and Survival in Cynomolgus Macaques. *J. Virol.* **2015**, *89* (13), 6773–6781.
- 365 (24) Carpenter, J. E.; Henderson, E. P.; Grose, C. Enumeration of an Extremely High Particle-to-PFU  
366 Ratio for Varicella-Zoster Virus. *J. Virol.* **2009**, *83* (13), 6917–6921.
- 367 (25) Flint, S. J.; Enquist, L. W.; Racaniello, V. R.; Skalka, and A. M. *Principles of Virology, 3rd Edition,*  
368 *Volume I: Molecular Biology*; ASM Press, 2009.
- 369 (26) Bettarel, Y.; Sime-Ngando, T.; Amblard, C.; Laveran, H. A Comparison of Methods for Counting  
370 Viruses in Aquatic Systems. *Appl. Environ. Microbiol.* **2000**, *66* (6), 2283–2289.
- 371 (27) Rossi, P.; Aragno, M. Analysis of bacteriophage inactivation and its attenuation by adsorption  
372 onto colloidal particles by batch agitation techniques. *Can. J. Microbiol.* **1999**, *45* (1), 9–17.
- 373 (28) Feng, Y. Y.; Ong, S. L.; Hu, J. Y.; Tan, X. L.; Ng, W. J. Effects of pH and temperature on the survival  
374 of coliphages MS2 and Q? *J. Ind. Microbiol. Biotechnol.* **2003**, *30* (9), 549–552.
- 375 (29) Carlson, G. F.; Woodard, F. E.; Wentworth, D. F.; Sproul, O. J. Virus Inactivation on Clay Particles  
376 in Natural Waters. *J. Water Pollut. Control Fed.* **1968**, *40* (2), R89–R106.
- 377 (30) Babich, H.; Stotzky, G. Reductions in inactivation rates of bacteriophages by clay minerals in lake  
378 water. *Water Res.* **1980**, *14* (2), 185–187.
- 379 (31) Trouwborst, T.; Kuyper, S.; De Jong, J. C.; Plantinga, A. D. Inactivation of some bacterial and  
380 animal viruses by exposure to liquid-air interfaces. *J. Gen. Virol.* **1974**, *24* (1), 155–165.
- 381 (32) Yeager, J. G.; O’Brien, R. T. Enterovirus inactivation in soil. *Appl. Environ. Microbiol.* **1979**, *38* (4),  
382 694–701.
- 383 (33) Chrysikopoulos, C. V.; Aravantinou, A. F. Virus inactivation in the presence of quartz sand under  
384 static and dynamic batch conditions at different temperatures. *J. Hazard. Mater.* **2012**, *233–234*,  
385 148–157.
- 386 (34) Küsel, K.; Totsche, K. U.; Trumbore, S. E.; Lehmann, R.; Steinhäuser, C.; Herrmann, M. How Deep  
387 Can Surface Signals Be Traced in the Critical Zone? Merging Biodiversity with Biogeochemistry  
388 Research in a Central German Muschelkalk Landscape. *Front. Earth Sci.* **2016**, *4*, 32.
- 389 (35) Kallies, R.; Kiesel, B.; Schmidt, M.; Kacza, J.; Ghanem, N.; Narr, A.; Zopfi, J.; Hackermüller, J.;  
390 Harms, H.; Wick, L. Y.; et al. Complete genome sequence of Pseudoalteromonas phage vB\_PS-  
391 H40/1 (formerly H40/1) that infects Pseudoalteromonas sp. strain H40 and is used as biological  
392 tracer in hydrological transport studies.
- 393 (36) Hijnen, W. A. M.; Brouwer-Hanzens, A. J.; Charles, K. J.; Medema, G. J. Transport of MS2 Phage,  
394 *Escherichia coli*, *Clostridium perfringens*, *Cryptosporidium parvum*, and *Giardia intestinalis* in a  
395 Gravel and a Sandy Soil. *Environ. Sci. Technol.* **2005**, *39* (20), 7860–7868.
- 396 (37) Aronino, R.; Dlugy, C.; Arkhangelsky, E.; Shandalov, S.; Oron, G.; Brenner, A.; Gitis, V. Removal of  
397 viruses from surface water and secondary effluents by sand filtration. *Water Res.* **2009**, *43* (1),  
398 87–96.
- 399 (38) Oppenheimer, C.; Zobell, C. The Growth and Viability of 63 Species of Marine Bacteria as  
400 Influenced. *J. Mar. Res.* **1952**, *11* (1), 10–18.
- 401 (39) Garza-Licudine, E.; Deo, D.; Yu, S.; Uz-Zaman, A.; Dunbar, W. B. Portable nanoparticle  
402 quantization using a resizable nanopore instrument-The IZON qNano™. In *Engineering in*

- 403 *Medicine and Biology Society (EMBC), 2010 Annual International Conference of the IEEE; IEEE,*  
404 *2010; pp 5736–5739.*
- 405 (40) Gutiérrez-Granados, S.; Cervera, L.; Segura, M. de las M.; Wölfel, J.; Gòdia, F. Optimized  
406 production of HIV-1 virus-like particles by transient transfection in CAP-T cells. *Appl. Microbiol.*  
407 *Biotechnol.* **2016**, *100* (9), 3935–3947.
- 408 (41) Arjmandi, N.; Van Roy, W.; Lagae, L. Measuring Mass of Nanoparticles and Viruses in Liquids with  
409 Nanometer-Scale Pores. *Anal. Chem.* **2014**, *86* (10), 4637–4641.
- 410 (42) Thompson, S. S.; Flury, M.; Yates, M. V.; Jury, W. A. Role of the air-water-solid interface in  
411 bacteriophage sorption experiments. *Appl. Environ. Microbiol.* **1998**, *64* (1), 304–309.
- 412 (43) Syngouna, V. I.; Chrysikopoulos, C. V. Transport of biocolloids in water saturated columns packed  
413 with sand: Effect of grain size and pore water velocity. *J. Contam. Hydrol.* **2011**, *126* (3–4), 301–  
414 314.
- 415 (44) Tufenkji, N.; Elimelech, M. Correlation Equation for Predicting Single-Collector Efficiency in  
416 Physicochemical Filtration in Saturated Porous Media. *Environ. Sci. Technol.* **2004**, *38* (2), 529–  
417 536.
- 418 (45) Sasidharan, S.; Torkzaban, S.; Bradford, S. A.; Kookana, R.; Page, D.; Cook, P. G. Transport and  
419 retention of bacteria and viruses in biochar-amended sand. *Sci. Total Environ.* **2016**, *548–549*,  
420 100–109.
- 421 (46) Rossi, P.; Dorfliger, N.; Kennedy, K.; Muller, I.; Aragno, M. Bacteriophages as surface and ground  
422 water tracers. *Hydrol. Earth Syst. Sci.* **1998**, *2* (1), 101–110.
- 423 (47) Flynn, R.; Hunkeler, D.; Guerin, C.; Burn, C.; Rossi, P.; Aragno, M. Geochemical influences on  
424 H40/1 bacteriophage inactivation in glaciofluvial sands. *Environ. Geol.* **2004**, *45* (4), 504–517.
- 425 (48) Frey, T. K. Molecular Biology of Rubella Virus. In *Advances in Virus Research*; Karl Maramorosch,  
426 F. A. M. and A. J. S., Ed.; Academic Press, 1994; Vol. 44, pp 69–160.
- 427 (49) Coffey, L. L.; Vignuzzi, M. Host Alternation of Chikungunya Virus Increases Fitness while  
428 Restricting Population Diversity and Adaptability to Novel Selective Pressures. *J. Virol.* **2011**, *85*  
429 (2), 1025–1035.
- 430 (50) Harvey, R. W.; Ryan, J. N. Use of PRD1 bacteriophage in groundwater viral transport, inactivation,  
431 and attachment studies. *FEMS Microbiol. Ecol.* **2004**, *49* (1), 3–16.
- 432 (51) Yeager, J. G.; O’Brien, R. T. Structural changes associated with poliovirus inactivation in soil. *Appl.*  
433 *Environ. Microbiol.* **1979**, *38* (4), 702–709.
- 434 (52) Jończyk, E.; Kłak, M.; Międzybrodzki, R.; Górski, A. The influence of external factors on  
435 bacteriophages—review. *Folia Microbiol. (Praha)* **2011**, *56* (3), 191–200.
- 436 (53) Dowd, S. E.; Pillai, S. D.; Wang, S.; Corapcioglu, M. Y. Delineating the specific influence of virus  
437 isoelectric point and size on virus adsorption and transport through sandy soils. *Appl. Environ.*  
438 *Microbiol.* **1998**, *64* (2), 405–410.
- 439 (54) Schijven, J. F.; Hassanizadeh, S. M. Removal of Viruses by Soil Passage: Overview of Modeling,  
440 Processes, and Parameters. *Crit. Rev. Environ. Sci. Technol.* **2000**, *30* (1), 49–127.
- 441 (55) Attinti, R.; Wei, J.; Kniel, K.; Sims, J. T.; Jin, Y. Virus’ (MS2, φX174, and Aichi) Attachment on Sand  
442 Measured by Atomic Force Microscopy and Their Transport through Sand Columns. *Environ. Sci.*  
443 *Technol.* **2010**, *44* (7), 2426–2432.
- 444 (56) Lasobras, J.; Muniesa, M.; Frías, J.; Lucena, F.; Jofre, J. Relationship between the morphology of  
445 bacteriophages and their persistence in the environment. *Water Sci. Technol.* **1997**, *35* (11), 129–  
446 132.
- 447 (57) Pecson, B. M.; Decrey, L.; Kohn, T. Photoinactivation of virus on iron-oxide coated sand:  
448 Enhancing inactivation in sunlit waters. *Water Res.* **2012**, *46* (6), 1763–1770.
- 449  
450

451

452

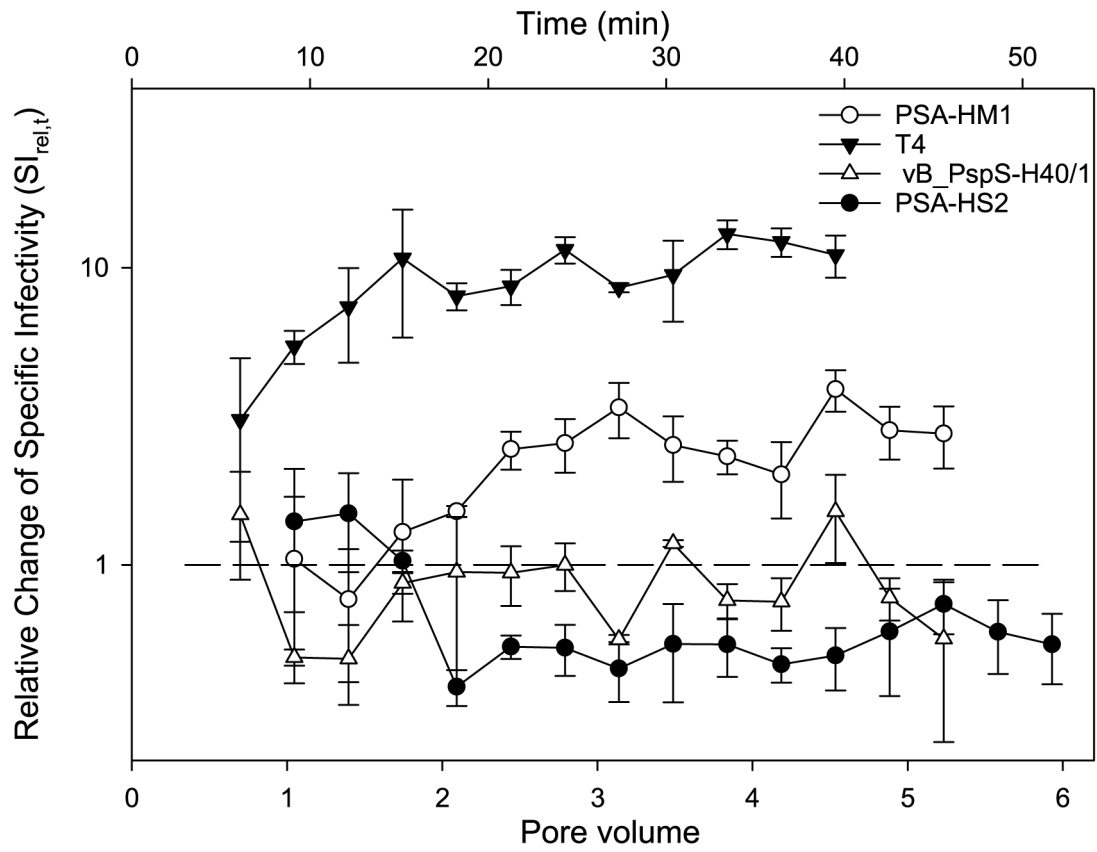


453

454 **Figure 1**

455

456



457

458 **Figure 2**

459

460

461

462